ATMOSPHERIC SCIENCE LETTERS
Atmos. Sci. Let. **12**: 176–183 (2011)
Published online 17 September 2010 in Wiley Online Library
(wileyonlinelibrary.com) **DOI:** 10.1002/asl.291

RMetS
Royal Meteorological Society

A comparison of the climate impacts of geoengineering by stratospheric SO_2 injection and by brightening of marine stratocumulus cloud

Andy Jones,* Jim Haywood and Olivier Boucher
Met Office Hadley Centre, FitzRoy Road, Exeter, EX1 3PB, UK

**Correspondence to:*
Andy Jones, Met Office Hadley Centre, FitzRoy Road, Exeter EX1 3PB, UK.
E-mail:
andy.jones@metoffice.gov.uk

Received: 22 January 2010
Revised: 23 July 2010
Accepted: 23 July 2010

Abstract

We examine the climate impact of geoengineering *via* two different methods, namely, stratospheric SO_2 injection and increasing reflectivity of marine stratocumulus clouds. Although both methods appear capable, in principle, of counteracting the global mean warming due to increases in greenhouse gas concentrations, significant changes in regional climate still result. The extent of this regional climate change appears linked to the location and degree of inhomogeneity of the radiative flux perturbations produced by each geoengineering method. © Crown Copyright 2010. Published with the permission of the Controller of HMSO and the Queen's Printer for Scotland

Keywords: **Geoengineering; climate change; regional climate**

1. Introduction

Alternatives to emission reduction have been proposed to counteract the effects of increases in concentrations of anthropogenic greenhouse gases (GHGs) or to directly reduce their concentrations through removal (Lenton and Vaughan, 2009; Royal Society, 2009). One subset of these 'geoengineering' proposals aims to manage the Earth's radiation budget by counteracting the positive radiative imbalance due to elevated GHG concentrations by reflecting solar radiation back to space.

Two proposed methods for increasing the Earth's reflectivity are (1) injection of sulphur dioxide (SO_2) into the stratosphere where it oxidises to form sulphate aerosol particles which scatter incoming sunlight (Crutzen, 2006) and (2) using automated ships to spray droplets of seawater into the marine boundary layer where they evaporate to form an elevated concentration of sea-salt aerosols which nucleate higher concentrations of cloud droplets in marine clouds, thereby increasing their reflectivity (Latham, 1990; Latham *et al*., 2008). We compare the climate impact of these two proposals simulated in the same coupled atmosphere–ocean climate model, based on the simulations of Jones *et al*. (2010) for stratospheric SO_2 injection and Jones *et al*. (2009) for marine cloud brightening. We assume that GHG concentrations rise in a 'business as usual' manner and that geoengineering is employed to counter the rise in temperature. We then assess the impact of geoengineering on future climate and how such a geoengineered world might differ from the current climate.

2. Model simulations

This study uses the second version of the Met Office Hadley Centre's Global Environment Model, HadGEM2-AO (Collins *et al*., 2008), which is a fully coupled atmosphere–ocean model. The atmosphere model has a horizontal resolution of 1.25° latitude by 1.875° longitude and has 38 vertical levels. The 40-level ocean/sea-ice model has a zonal resolution of 1° throughout and a variable meridional resolution: 1° from the Poles to 30 °N/S, then increasing smoothly to 1/3° at the equator. The one small difference between the model used by Jones *et al*. (2009) for cloud brightening and that used by Jones *et al*. (2010) for stratospheric SO_2 injection is the introduction of gravitational sedimentation of sulphate aerosol in the latter. This process is insignificant in the troposphere where sulphate removal is dominated by wet deposition, but when simulating stratospheric sulphate this process must be included to ensure a realistic aerosol lifetime.

To estimate the impact of geoengineering on the radiative balance of the Earth, we used the atmosphere-only version of this model, where prescribed sea-surface temperatures and sea-ice distributions appropriate for the late 20th century are used. Two pairs of simulations are performed, one simulation in each pair being a control, the other with geoengineering. The 10-year mean difference in top-of-atmosphere net radiation provides a measure of the radiative impact of the respective geoengineering methods. As each simulation in a pair evolves with different meteorology, the radiative impact is not a true radiative forcing but a measure known as the radiative flux perturbation (RFP) (Haywood *et al*., 2009).

The climate response to geoengineering was investigated using the fully coupled model. For each geoengineering method, we consider three simulations: (1) a 'Control' simulation up to 2000 driven by historical forcings; (2) a 60-year 'A1B' simulation initialised from 2000 with GHG emissions following the IPCC's A1B scenario (Nakićenović *et al.*, 2000); and (3) a 60-year 'A1B + geoengineering' simulation. Geoengineering could be introduced gradually so that global mean temperatures do not deviate much from current values. How such a phasing-in might be calibrated is currently unknown, and we therefore performed idealised simulations where geoengineering was applied fully from 2000.

For geoengineering *via* stratospheric SO_2 injection, we use the simulations of Jones *et al.* (2010) which follows Robock *et al.* (2008) injecting 2.5 Tg[S] $year^{-1}$ into the lower stratosphere (~16–23 km). The standard version of HadGEM2 (model top at ~40 km) is not a dedicated 'stratospheric' configuration, so to reduce any problems with stratospheric transport, SO_2 injection was applied uniformly across the globe. For geoengineering *via* cloud brightening, we use the 'ALL' simulations of Jones *et al.* (2009), which modifies the persistent stratocumulus cloud sheets on the eastern sides of the North Pacific, South Pacific and South Atlantic by increasing cloud droplet number concentration to the model's asymptotic limit of 375 cm^{-3}.

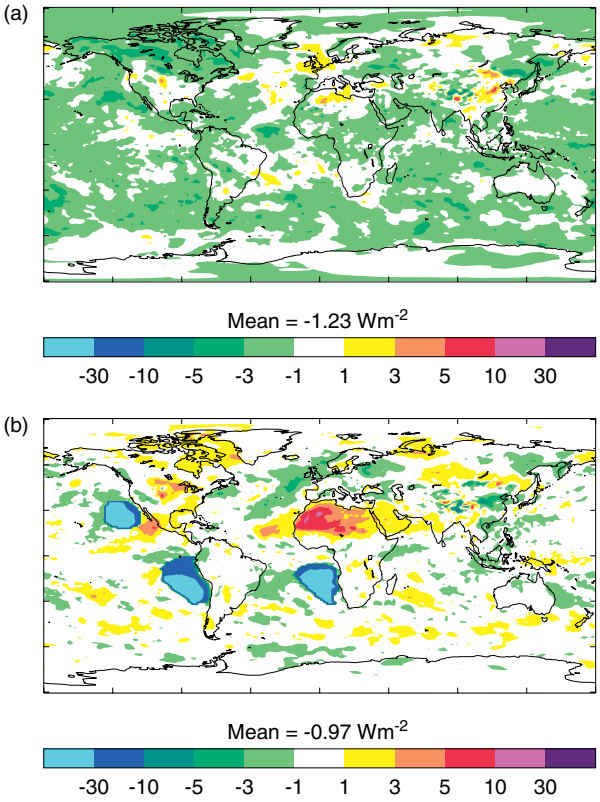

Figure 1. Annual mean radiative flux perturbation (Wm^{-2}) for geoengineering *via* (a) stratospheric SO_2 injection at 2.5 Tg[S] $year^{-1}$, and (b) increasing cloud droplet concentration to 375 cm^{-3} in the marine stratocumulus cloud sheets at the eastern sides of the North Pacific, South Pacific and South Atlantic.

3. Results

3.1. Radiative flux perturbation

Figure 1 shows the distribution of 10-year mean RFP from stratospheric SO_2 injection (Figure 1(a)) and marine stratocumulus cloud brightening (Figure 1(b)). The global mean RFP from SO_2 injection is approximately 25% greater than that from cloud brightening for the scenarios presented here, but both are significant compared with the positive forcing due to current levels of GHGs (+2.63 Wm^{-2}; IPCC, 2007). Their geographic distributions, however, are completely different. The RFP from SO_2 injection is quite uniformly distributed, with local values rarely exceeding −3 Wm^{-2}. In contrast, the RFP from cloud brightening is concentrated solely in the areas of marine stratocumulus, with values of more than −30 Wm^{-2} over much of these regions. This extreme inhomogeneity is of course related to the experimental design which targets the stratocumulus regions. The area of positive RFP over the Sahara in Figure 1(b) is due to a difference in mineral dust concentration between experiment and control simulations. Whether this is causally related to the cloud modification or a random fluctuation in this highly variable quantity is a topic for further study.

3.2. Climate impacts of SO_2 injection

For geoengineering *via* stratospheric SO_2 injection, Figure 2(a) shows the time evolution of annual global mean near-surface air temperature for the period 1990–1999 in the Control (green line) simulation, and for A1B (red line) and A1B + geoengineering (blue line) simulations for 2000–2060. As geoengineering is applied fully from 2000 the A1B + geoengineering simulation cools initially, but the effect of GHG increases eventually dominates. Warming recommences after about 20 years, reaching late 20th century values after ~35 years.

We consider averages of three decades as shown in Figure 2(a): years 1990–1999 in the Control, an approximate measure of current climate (decade A); the years 2028–2037 in the geoengineering simulation, where the decadal mean temperature difference from decade A is approximately zero (decade B); and the same period as B but in the A1B run (decade C). The climate in decade B might depend on the trajectory of the simulation before the period in question – for example, it might be different if geoengineering could have kept the temperature constant at the 1990–1999 level. Jones *et al.* (2010) performed another simulation where geoengineering was terminated in 2025. This warmed to the 1990–1999 level faster than the standard geoengineering simulation, yet

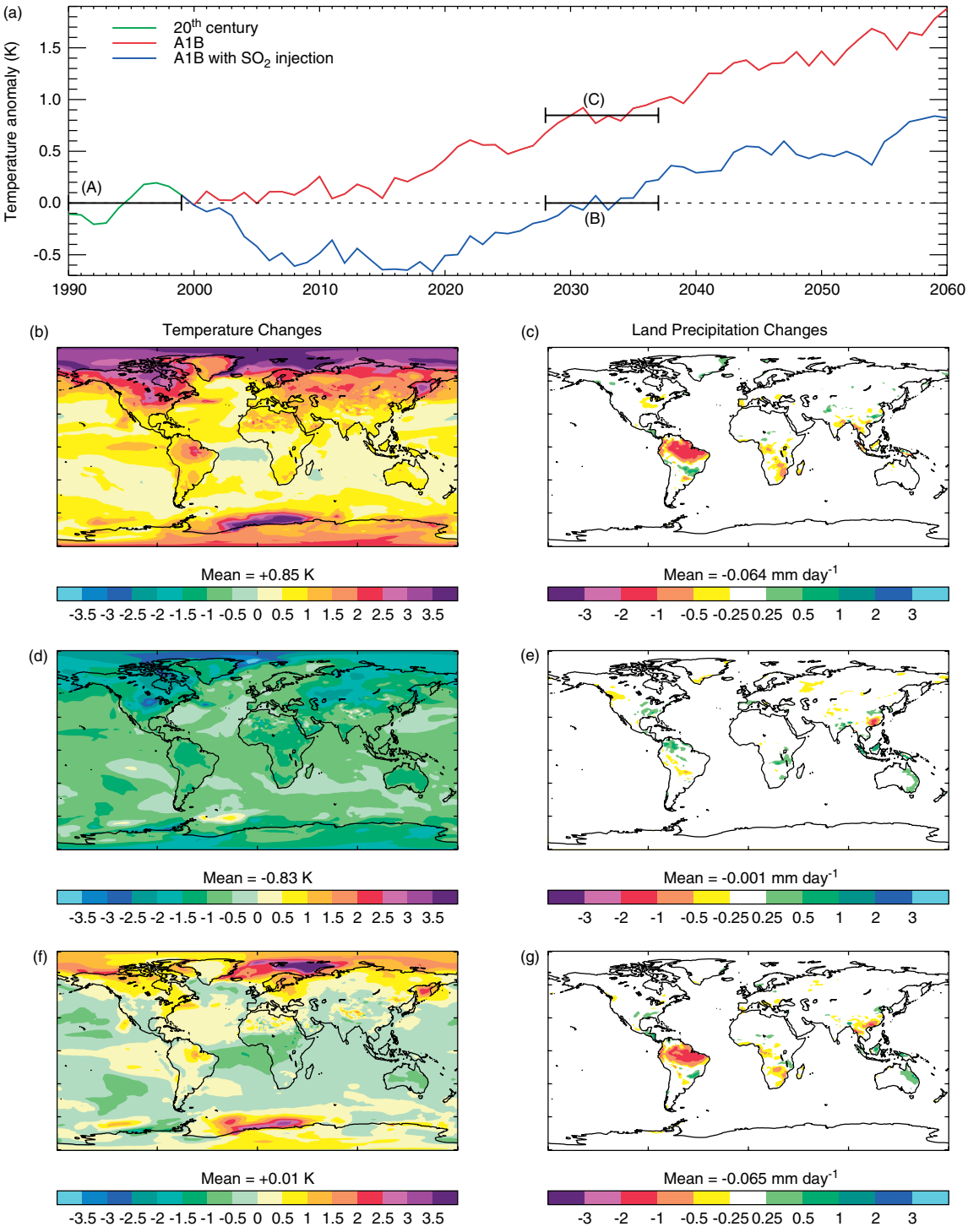

Figure 2. Climate impacts of geoengineering *via* stratospheric SO_2 injection. (a) Evolution of annual global mean 1.5 m air temperature anomaly (K) with respect to the 1990–1999 period (decade A). (b) Change in 1.5 m air temperature (K): decade C minus decade A. (c) Change in land precipitation rate (mm day^{-1}): decade C minus decade A. (d) As (b) but for B minus C. (e) As (c) but for B minus C. (f) As (b) but for B minus A. (g) As (c) but for B minus A.

the climate in this period was very similar to that in decade B, suggesting that the precise trajectory to decade B may not be relevant. This may not hold, however, for changes on longer timescales or if the change is so large as to trigger some irreversible feedback.

We first consider how climate might change under the A1B scenario without any geoengineering. This provides a baseline against which to assess the effects of geoengineering. The impact of A1B at the given period is shown in Figure 2(b) and (c) for annual mean near-surface air temperature and land precipitation, respectively; this is the difference between decades C and A (Figure 2(a)). The changes in temperature follow the classic signal of GHG-induced warming (IPCC, 2007) with greater warming at high latitudes and over land. Global mean precipitation changes by

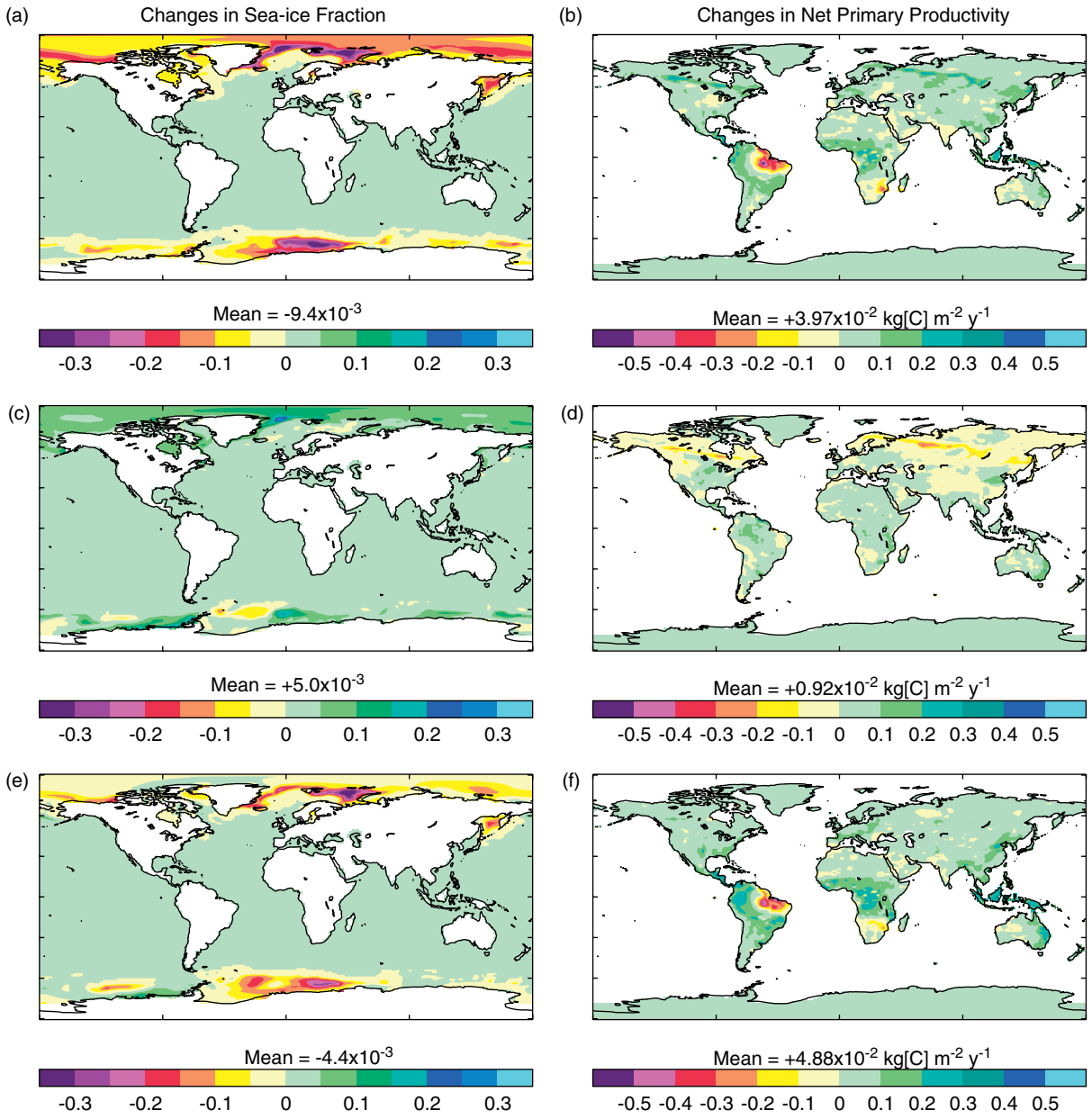

Figure 3. Changes in annual mean sea-ice fraction (left column) and net primary productivity (right column, kg[C] m^{-2} $year^{-1}$) for geoengineering *via* stratospheric SO_2 injection: (a) and (b), impact of A1B – decade C minus decade A; (c) and (d), impact of geoengineering – decade B minus decade C; (e) and (f), combined impact for no change in global mean temperature – decade B minus decade A.

−0.5% and there is also a net reduction in land precipitation, with large reductions in Amazonia and smaller reductions in southern Africa and around the Bay of Bengal. The impact on sea-ice and vegetation net primary productivity (NPP) is shown in Figure 3(a) and (b), respectively. Arctic and Antarctic sea-ice areas reduce by approximately 3.2 and 1.8 million km^2, respectively, relative to the 1990–1999 mean values (Arctic, 18.8, and Antarctic, 11.5 million km^2). The effects of CO_2 fertilization produce a general increase in NPP (Figure 3(b)), with the clear exception of the northeastern region of South America.

The impact of geoengineering on the GHG-induced warming is shown in Figure 2(d), which is the difference between decades B and C. The distribution of cooling is similar to the warming produced by GHGs, with more cooling at high latitudes and over land. Global mean precipitation is reduced by 1.8%, although there is little impact on precipitation over land (Figure 2(e)): while the distribution of changes generally tends to oppose that due to GHG increases, they are much smaller in magnitude. Figure 3(c) shows that the cooling restores some of the sea-ice, increasing by approximately 1.8 and 0.9 million km^2 in the Arctic and Antarctic, respectively. The impact on NPP is small (Figure 3(d)).

Finally, the climate changes in a geoengineered world compared with current conditions are indicated by the differences between decades B and A. By design the change in global mean temperature

with respect to current levels is ~0, but regionally there are significant differences (Figure 2(f)). There are large areas of cooling, with central Africa and Australia being more than 0.5 K cooler than current levels. However, there is significant high latitude warming, especially in the Arctic, where warming exceeds 3 K over a considerable area. Figure 3(e) shows that the impact of GHGs still dominates the changes in sea-ice, with reductions at both Poles compared with 1990–1999 levels. Global mean precipitation is reduced by approximately 2.3% from 3.05 to 2.98 mm day^{-1}, and the large reduction in precipitation over Amazonia is still evident (Figure 2(g)), which would have serious consequences for the rainforest, as indicated by the impact on NPP (Figure 3(f)). On the other hand, there is a general increase in NPP in other tropical areas, including sub-Saharan Africa.

3.2. Climate impacts of stratocumulus modification

Figure 4(a) shows the time evolution of near-surface air temperature for the case of geoengineering *via* marine stratocumulus modification. The Control simulation is the same as in Figure 2(a), and while the A1B run is a slightly different realization of that shown in Figure 2, as the latter includes a treatment of the gravitational sedimentation of sulphate aerosol, they are in all relevant respects the same.

As the RFP from stratocumulus modification is about 25% smaller than that from SO_2 injection, global mean temperature in the geoengineering run returns to the 1990–1999 mean value somewhat earlier, so decades B and C are now years 2019–2028 (Figure 4(a)). As decade B is now ~10 years earlier than for SO_2 injection, the impacts of GHG increases in A1B (Figure 4(b) and (c)) are somewhat smaller than the corresponding panels in Figure 2, but the distributions are very similar. The same applies to the impacts on sea-ice (Figure 5(a)) and NPP (Figure 5(b)); at this point in time, Arctic and Antarctic sea-ice cover in A1B have been reduced by 2.3 and 1.3 million km^2, respectively.

The impact on near-surface temperature is shown in Figure 4(d) (difference of decades B and C). The cooling is more inhomogeneous than in the case of SO_2 injection, with areas of strong cooling in the vicinity of the three persistent stratocumulus sheets. There are also larger areas which show some warming, the northeast of South America being one notable region. There is less of a positive impact on sea-ice, with increases of 0.9 and 0.5 million km^2 in Arctic and Antarctic sea-ice cover, respectively. Global mean precipitation is reduced by 1.6%, but the changes in land precipitation (Figure 4(e)) are significantly different from those caused by SO_2 injection (*cf.* Figure 2(e)), with a large area of South America showing a marked reduction in precipitation. This feature is also seen in the change in NPP (Figure 5(d)).

The distribution of temperature changes in the geoengineered world is shown in Figure 4(f). Despite there being no change in the global mean temperature, there are marked regional changes. As in Figure 2(f), there is significant warming at high latitudes and cooling at low latitudes, but the latter is stronger in the case of stratocumulus modification. There is also more continental warming in the Northern Hemisphere and increased warming in the north of South America. As with SO_2 injection, there are significant reductions in polar ice (Figure 5(e)). Global mean precipitation is reduced by 2.3% as in the SO_2 simulations, but the changes in land precipitation are greater than for SO_2 injection with enhanced drying in South America (Figure 4(g)) and consequent impacts on NPP (Figure 5(f)).

4. Discussion and Conclusion

Both geoengineering methods are successful in counteracting the rise in global mean temperature caused by increasing concentrations of GHGs, at least for a time. To continue to balance the GHG-induced warming after their respective B decades, the level of geoengineering would have to be increased. For SO_2 injection, this would mean having to increase injection rates, although possible nonlinear effects could reduce the cooling efficiency of further injection (Heckendorn *et al*., 2009). For the cloud brightening approach, this would presumably entail further cloud modification, in terms of increasing both the regions where clouds were modified and the amount by which they were modified. For either approach to geoengineering, the problems that would arise should geoengineering suddenly be terminated would only increase as time went on.

Although there is no change in global mean temperature in the B decades of the geoengineering simulations, the same is not true for global mean precipitation, both methods producing a reduction of 2.3%, comparable with the 1.7% reduction for a similar scenario obtained by Bala *et al*. (2008). As discussed by Bala *et al*. (2008), this illustrates one of the problems in attempting to counteract the longwave radiative impact of GHGs by changing the planet's shortwave radiation balance.

The impact of geoengineering on regional climate for the two cases considered here has a strong dependence on the homogeneity and/or location of the applied RFP. Despite the somewhat larger RFP (-1.3 *cf.* -1.0 Wm^{-2}), the negative impacts of (uniform) SO_2 injection are arguably less than those due to (regional) stratocumulus modification. For SO_2 injection, the distribution of cooling is similar to the GHG-induced warming, and the changes in land precipitation, while small, generally tend to oppose those induced by GHGs. In contrast, the temperature and precipitation changes caused by stratocumulus modification are quite different, and in the case of South America, act to enhance, not reduce, both

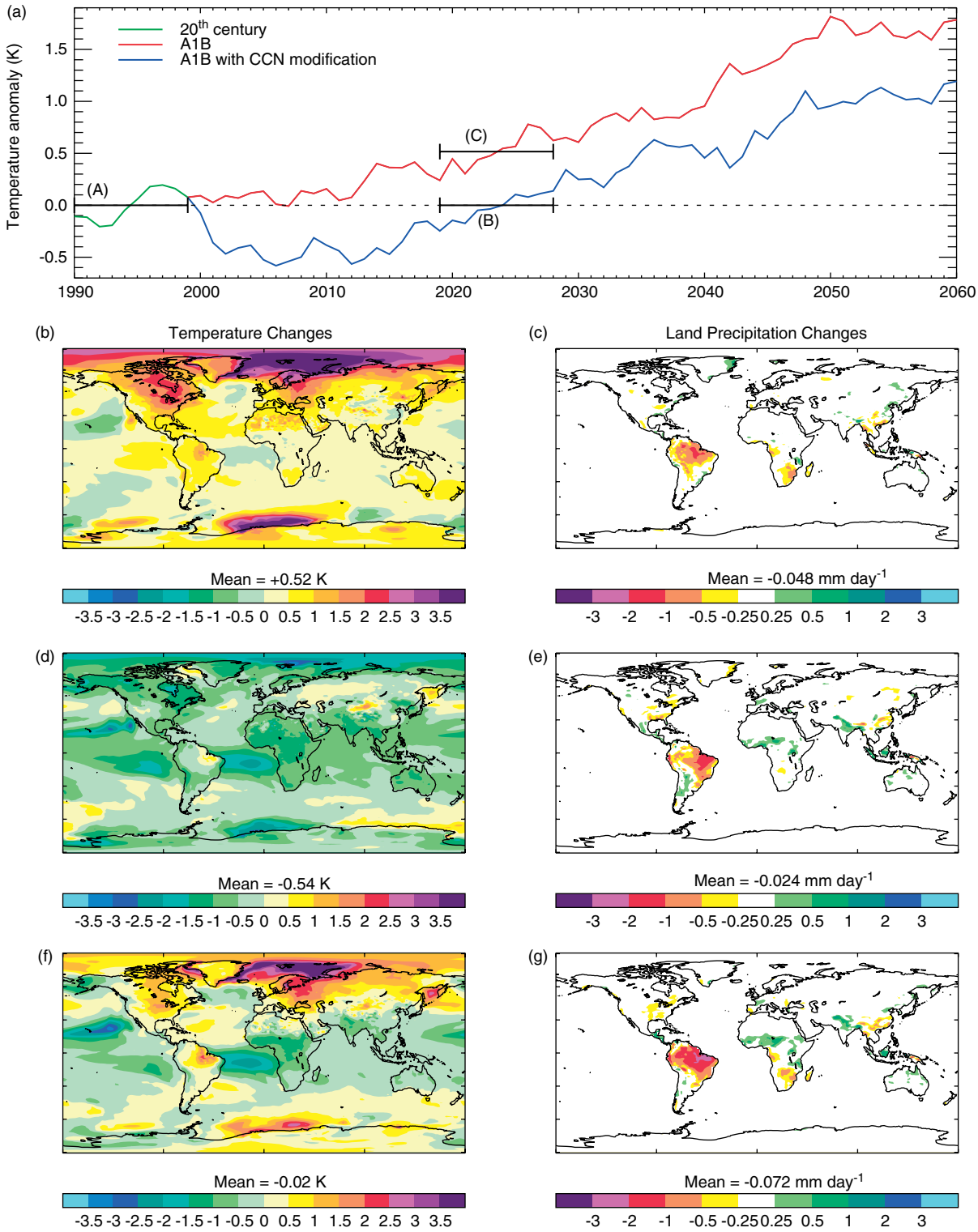

Figure 4. As Figure 2 but for the climate impacts of geoengineering *via* marine stratocumulus modification. Note that decades B and C are earlier than in Figure 2 (2019–2028 *cf.* 2028–2037).

the warming and the drying caused by GHGs. It would, of course, be possible to modify clouds in other areas, and to a different degree than investigated by Jones *et al.* (2009). Rasch *et al.* (2009) modified clouds over 20–70% of the world's oceans, compared with the <5% of ocean area considered here. They also increased cloud droplet number concentration to much higher values (1000 cm^{-3} compared with 375 cm^{-3}). The results of Rasch *et al.* (2009) do not show a significant reduction of precipitation over South America, although it is not clear whether this is due to differences in experimental design or to the different behaviour of the two climate models. The semi-permanent marine stratocumulus cloud sheets considered by Jones *et al.* (2009) are likely the best year-round areas to apply geoengineering

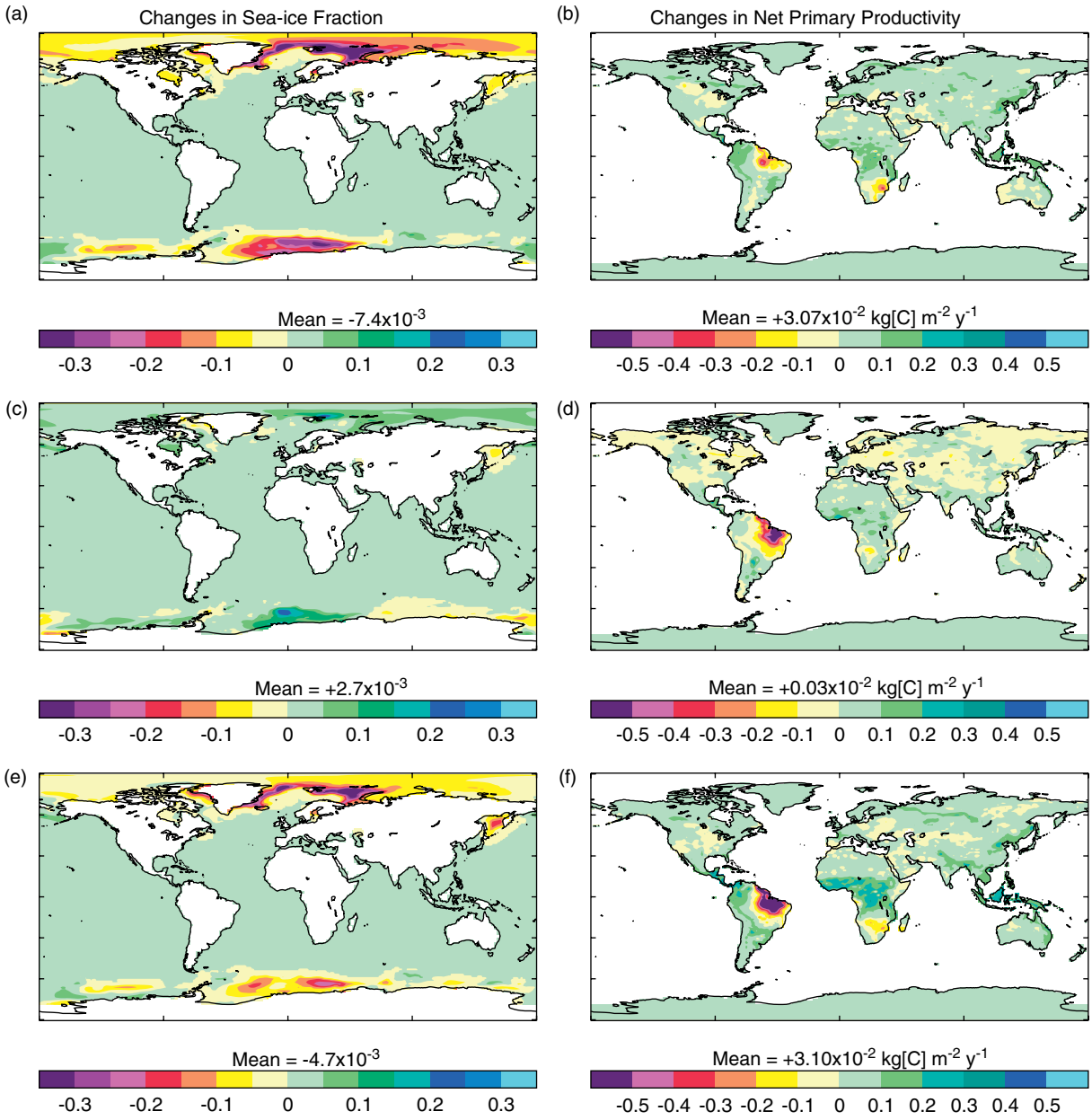

Figure 5. As Figure 3 but for geoengineering *via* marine stratocumulus modification. Note that decades B and C are earlier than in Figure 3 (2019–2028 *cf.* 2028–2037).

(Salter *et al.*, 2008). Not only are the cloud's radiative properties and lifetime sensitive to perturbation by geoengineering, but the lifetime of sea-salt in the atmosphere subsequent to injection is longer than elsewhere owing to reduced precipitation. Model simulations show that sea-salt aerosol lifetimes are three to six times longer in the stratocumulus areas compared with mid-latitude storm-track regions.

The main conclusion is that using geoengineering to maintain the global mean temperature at current levels is unlikely to avoid significant regional climate changes due to continued increases in GHG concentrations: the regional changes caused by longwave radiative forcing by GHGs cannot be simply offset by invoking a compensating shortwave forcing through geoengineering. The nature and distribution of the response to geoengineering appears to depend on the distribution of the applied forcing, and it may prove a challenge to understand these regional climate responses.

Acknowledgements

This work was supported by the Joint DECC and Defra Integrated Climate Programme – DECC/Defra (GA01101).

References

Bala G, Duffy PB, Taylor KE. 2008. Impact of geoengineering schemes on the global hydrological cycle. *Proceedings of the National Academy of Sciences* **105**: 7664–7669.

Collins WJ, *et al.* 2008. Evaluation of the HadGEM2 model. *Hadley Centre Technical Note 74*. Met Office, Exeter, UK. Available at http://www.metoffice.gov.uk/publications/HCTN/index.html.

Crutzen P. 2006. Albedo enhancement by stratospheric sulfur injections: a contribution to resolving a policy dilemma?. *Climatic Change* **77**: 211–219. DOI: 10.1007/s10584-006-9101-y.

Haywood J, Donner L, Jones A, Golaz J-C. 2009. Global indirect radiative forcing caused by aerosols: IPCC (2007) and beyond. In *Clouds and the Perturbed Climate System: Their Relationship to Energy Balance, Atmospheric Dynamics and Precipitation*, 451–467, J Heintzenberg, RJ Charlson (eds). Strüngmann Forum Report, MIT Press: Cambridge, USA.

Heckendorn P, Weisenstein D, Fueglistaler S, Luo BP, Rozanov E, Schraner M, Thomason LW, Peter T. 2009. The impact of geoengineering aerosols on stratospheric temperature and ozone. *Environmental Research Letters* **4**: 045108. DOI: 10.1088/1748-9326/4/4/045108.

IPCC. 2007. *Climate Change 2007: The Physical Science Basis. Contribution of Working Group I to the Fourth Assessment Report of the Intergovernmental Panel on Climate Change*, S Solomon *et al*. (eds). Cambridge University Press: Cambridge, UK.

Jones A, Haywood J, Boucher O. 2009. Climate impacts of geoengineering marine stratocumulus clouds. *Journal of Geophysical Research* **114**: D10106. DOI: 10.1029/2008JD011450.

Jones A, Haywood J, Boucher O, Kravitz B, Robock A. 2010. Geoengineering by stratospheric SO_2 injection: results from the Met Office HadGEM2 climate model and comparison with the Goddard Institute for Space Studies ModelE. *Atmospheric Chemistry and Physics* **10**: 5999–6006. DOI: 10.5194/acp-10-5999-2010.

Latham J. 1990. Control of global warming?. *Nature* **347**: 339–340.

Latham J, Rasch P, Chen C-C, Kettles L, Gadian A, Gettelman A, Morrison H, Bower K, Choularton T. 2008. Global temperature stabilization via controlled albedo enhancement of low-level maritime clouds. *Philosophical Transactions of the Royal Society A* **366**: 3969–3978. DOI: 10.1098/rsta.2008.0137.

Lenton TM, Vaughan NE. 2009. The radiative forcing potential of different climate geoengineering options. *Atmospheric Chemistry and Physics* **9**: 5539–5561.

Nakićenović N, Alcamo J, Davis G, de Vries B, Fenhann J, Gaffin S, Gregory K, Grübler A, Jung TA, Kram T, Lebre La Rovere E, Michaelis L, Mori S, Morita T, Pepper W, Pitcher H, Price L, Riahi K, Roehrl A, Rogner H-H, Sankovski A, Schlesinger M, Shukla P, Smith S, Swart R, van Rooijen S, Victor N, Dadi Z. 2000. *IPCC Special Report on Emission Scenarios*. Cambridge University Press: Cambridge,UK.

Rasch PJ, Latham J, Chen C-C. 2009. Geoengineering by cloud seeding: influence on sea ice and climate system. *Environmental Research Letters* **4**: 045112. DOI: 10.1088/1748-9326/4/4/045112.

Robock A, Oman L, Stenchikov GL. 2008. Regional climate responses to geoengineering with tropical and Arctic SO_2 injection. *Journal of Geophysical Research* **113**: D16101. DOI: 10.1029/2008JD010050.

Royal Society. 2009. *Geoengineering the Climate: Science, Governance and Uncertainty*. RS policy document 10/09, The Royal Society: London, UK; 82.

Salter S, Sortino G, Latham J. 2008. Sea-going hardware for the cloud albedo method of reversing global warming. *Philosophical Transactions of the Royal Society A* **366**: 3989–4006. DOI: 10.1098/rsta.2008.0136.